

Mimics Based Image Reconstruction Augments Diagnosis and Management of Vascular Pathologies: A Study of Ruptured Abdominal Aortic Aneurysms

Michalis Xenos¹, Suraj Rambhia¹, Yared Alemu¹, Shmuel Einav¹, John J. Ricotta^{2,3}, Nicos Labropoulos³, Apostolos Tassiopoulos³, and Danny Bluestein¹

¹Department of Biomedical Engineering, Stony Brook University, Stony Brook, NY

²Department of Surgery, Washington Hospital Center, Washington, DC

³Department of Surgery, Stony Brook University Hospital, Stony Brook, NY

Abstract:

Societal Relevance: Cardiovascular pathology is the leading cause of death and disability in the Western World. Rupture of abdominal aortic aneurysm (AAA), having a mortality rate of 50-75%, ranks as the 13th leading cause of death in the US. The ability to reliably predict the risk of rupture of AAA on a patient-specific basis could vastly improve the clinical management of these patients. The anatomic conditions that predispose to aneurismal dilation of the aorta are present to varying degrees in the majority of the Western population over age 50. Current diagnostic tests (CT / MR angiography and duplex ultrasound) can identify the existence of aneurysm pathology with a high degree of sensitivity, but are not specific enough to identify patients at high risk for disease progression and rupture. With the advances in computer graphics techniques for surface rendering, the potential for extracting valuable information from these modalities has emerged. Combining these modalities with advanced numerical simulations additionally facilitates the quantification of significant clinical parameters that offer enhanced diagnosis of the patient's condition, and can be used to arrive to a better informed decision regarding the need for a surgical intervention.

Innovation: High risk aneurysms that are candidates for surgical intervention are those with aneurismal diameter larger than 5.5cm. This size-based-criterion fails to differentiate between small diameter aneurysms with high risk of rupture and large diameter aneurysms that may be stable. To provide a way of quantifying the risk of rupture of AAAs, we introduced a methodological approach for developing a patient specific diagnostic tool of abdominal aortic aneurismal disease integrating elaborate medical imaging with advanced numerical modeling. The proposed methodology incorporates advanced constitutive material models of the various components of AAA in fluid structure interaction (FSI) simulations, including effects of anisotropy (structural strength based on collagen fibers orientation within the arterial wall), AAA intraluminal thrombus (ILT), and embedded calcifications. We incorporate in the methodology relevant clinical parameters obtained during prospective studies into patient-specific reconstructed models, including flow velocities measured by Doppler ultrasound and non-uniform wall thickness detection. In a ground breaking study of ruptured abdominal aortic aneurysms (AAAs), with the use of Mimics, a state-of-the-art image reconstruction tool, we simulate the interaction of blood with the anisotropic vessel wall, including important structures of the AAA pathology such as the intraluminal thrombus (ILT) and calcified spots.

Economical potential: The developed methodology will lead to characterization of AAA geometric features, including: shape, length to traverse dimensions ratios, neck and iliac arteries angulation, tortuosity, wall thickness and strength, calcifications. The developed models are capable of predicting the rupture potential of AAAs based on wall stress mapping, incorporating wall strength estimations based on biomechanical and clinical parameters. The potential of such a non-invasive diagnostic tool, starting with Mimics in image reconstruction, certainly will be indispensable for physicians and scientists in quantifying the risk of rupture in AAAs. Such diagnostic capabilities are essential for improved clinical outcomes of procedures in which intervention is directed at those lesions most likely to become symptomatic. This methodology will be readily applicable for analyzing and diagnosing other cardiovascular pathologies, such as vulnerable plaques in carotid and coronary arteries. By refining the indications for elective surgery and eliminating unnecessary or low benefit surgery, the clinical endpoint will improve surgical outcomes, reduced mortality rates, and considerable savings in healthcare costs.

1. Introduction

Abdominal aortic aneurysms (AAAs) comprise a class of vascular pathology that manifests in a remodeling of the abdominal aorta. AAAs are most common in patients who have a history of coronary, carotid, or peripheral vascular disease, a history of smoking, or family history of aneurismal disease. It is suggested that both males over 65 years of age and high-risk females receive prophylactic screening or treatment. Due to a globally aging population, the incidence of AAAs is increasing along side medical costs associated with patient management¹⁻⁴. In 2003 alone, more than 154.7 million dollars comprised the monetary costs of electrocardiography, endovascular and non-invasive diagnostic imaging procedures used for management of AAAs in the U.S. Complications of AAA, usually rupture of the pressurized bulge in the abdominal aorta, ultimately leads to death in 50-75% of rupture cases^{5,6}, despite the use of highly advanced imaging techniques such as computed tomography (CT), magnetic resonance (MR) imaging, and duplex ultrasound.

The high mortality rate seen in cases of ruptured AAAs can be attributed, in part, to the anatomical location of the abdominal aorta just rostral to the iliac and caudal to the renal arterial bifurcations. However, endovascular correction in cases of abdominal aortic aneurysms is tempered by the high risk of this type of operation. In general, endovascular correction is performed only when the risk of rupture is greater than the risk of the operation. Determination of the risk of rupture of AAAs, thus, follows as an important juncture in patient management to ascertain whether or not the vascular surgeon should perform endovascular correction. The problem lies in current protocols for determining the risk of rupture. Using a size based criterion, endovascular surgery is likely to be performed if the aneurismal bulge diameter exceeds 5.0 to 5.5 cm^{5,6}. The size based criterion does not provide any information on how the surgery should be performed and often misrepresents the multifactorial nature of actual risk of rupture⁷. Currently, there is no means of measuring, *in-vivo*, the wall stresses or tissue strength of the aneurysm, but computational models are able to calculate fluid and solid properties and can better assist in ascertaining the risk of rupture.

Fillinger et al.⁸ have shown that computational models using a static uniform internal pressure on a AAA can be 12% more accurate and 13% more sensitive than using maximum diameter as a sole predictor for risk of rupture. Several other studies have used idealized geometries to measure the effects of variations in wall thickness and the presence or absence of intraluminal thrombus (ILT) formations. A uniaxial tensile test to develop a hyperelastic isotropic constitutive relation for the ILT was developed by the Vorp group⁹. The developed framework showed the ILT, one of the known pathologic features seen in AAAs, to be heterogeneously composed of three distinct layers with different mechanical properties. With the aid of three-dimensional image reconstruction tools, such as Mimics, one can link subsets of reconstructed patient data to the various material properties defined in aforementioned computational models in an effort to develop a robust methodology for quantitative assessment of the risk of rupture of AAAs. The level of accuracy obtained from fusing patient data with computational models would be determined by the accuracy of the computational model, the detail of the reconstructed anatomical structure, as well as the computational power available.

Outline: In this study, we apply a novel proof-of-concept methodology to patient specific CT data to obtain quantitative information concerning the biomechanics of AAAs that may lead to rupture, based on information extracted from the Mimics imaging software. Section two presents a schematic diagram of the overall methodology utilized to achieve the objectives of this study. Section three describes the image reconstruction in Mimics, utilized to retain anatomical complexity from contrast CT scans. Section four presents the computational fluid dynamics approach and results from simulations in Fluent. In Section five, we introduce the fluid structure interaction methodology. Results are discussed with details of the computational models utilized in subsequent

numerical simulations. Finally, section six summarizes the role of Mimics in establishing a quantitative assessment of risk of rupture in AAAs.

2. Methods: Patient Specific Approach for Fluid-Structure Interaction

The approach to perform patient specific dynamical analysis between fluid and solid structures in pathological AAAs is described in Figure 1 and is composed of five stages. Initially, imaging data was acquired through a standard clinical approach like computed tomography (CT). Informed consent was obtained retrospectively for all studied cases. The protocol was approved by Stony Brook University Institutional Review Board (IRB) Committees on Research Involving Human Subjects.

Boundaries of reconstruction were established for the section of the abdominal aorta. Most commonly, the lower boundary was established just beyond the iliac bifurcation, and the upper boundary was set around the region where renal arteries branch off the abdominal aorta. This allowed for proper observation of the AAA pathology. Using Mimics (Mimics, Materialise, Leuven, Belgium) image reconstruction software¹⁰, we reconstruct the anatomical details of the vessel, like the outer wall, lumen, intraluminal thrombus (ILT), and calcifications using different layered masks.

In a normal abdominal aorta, the outer wall is a reinforced fibrous material, which surrounds the blood carrying lumen. Due to vessel remodeling in pathological scenarios, a ballooning of the outer wall is observed in cases of AAA. This remodeling can result from the combined effects of hardened calcified spots and the presence of a soft, fatty intraluminal thrombus. Exporting the three-dimensionally rendered geometry in STL format or polylines in IGES format is a simple and robust process. The reconstructed surfaces were then imported into a computational fluid dynamics (CFD) preprocessing software tool, to allow for the generation of a computational mesh¹¹. The three-dimensional geometry rendered in Mimics was discretized into thousands of smaller triangular surface elements for further CFD analysis or fluid structure interaction (FSI) simulations^{12, 13}.

CFD was performed in Fluent (Fluent, Ansys Inc, Lebanon, NH) with the fluid modeled as blood and static walls. FSI, performed in Adina (Adina, ADINA R&D Inc, Watertown, MA), goes one step further to assess the interaction of the fluid and solid domains. The fluid domain was modeled as blood. However, the solid domain in our formulation was composed of three parts, the

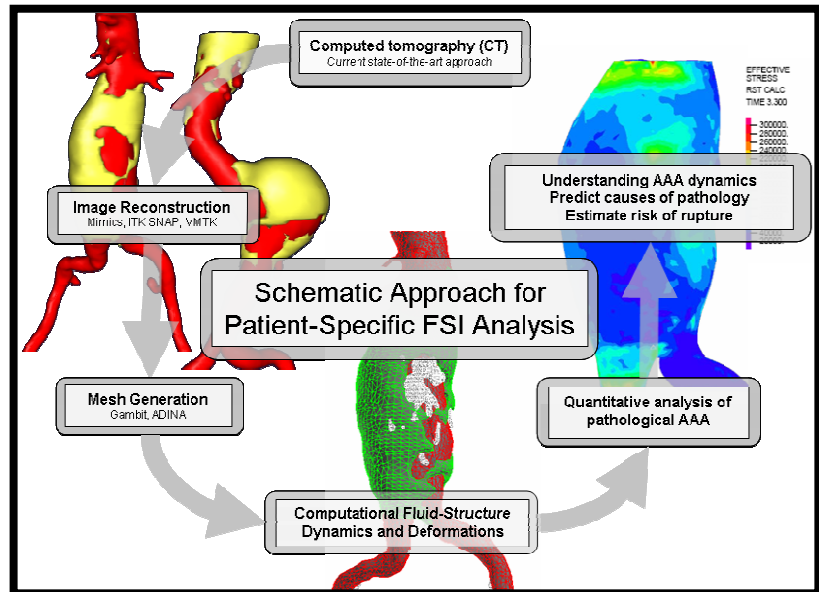


Figure 1. Schematic diagram of patient specific fluid structure interaction (FSI) approach shows the main stages through which conventional patient CT data is used for estimating risk of rupture in AAAs. (i) Acquiring of imaging data with contrast through standard clinical approaches. (ii) Reconstruction of abdominal aorta beyond iliac bifurcation for proper observation of AAA pathology using Mimics image reconstruction software. (iii) Discretization of geometry to generate a computational mesh in Gambit. This mesh is then exported to Fluent for computational fluid dynamics (CFD) analysis or to Adina for FSI analysis. (iv) CFD and FSI can be used to provide surgeons with quantitative information to assess the risk of rupture of AAAs.

vessel wall, ILT, and calcifications. Modeling the solid vessel structure involved mathematical description of the fiber orientation as an orthotropic material formulation. Using an orthotropic model, the fiber orientation of the solid vessel wall was determined based on fitting simulated data to published experimental results in AAA cases^{14, 15}. The quantitative information acquired from CFD and FSI through this approach can be used to provide surgeons with quantitative information to assess the risk of rupture of AAAs. In the following section, we provide a description of the image reconstruction procedure in Mimics with some representative ruptured AAA cases.

3. Image Reconstruction: Three-Dimensional Rendering of AAA Geometries

Contrast CT images were used to reconstruct ruptured AAA geometries. Layered masks were automatically segmented in Mimics software with some manual adjustment. Because of the difficulty encountered when discerning between soft tissue boundary of the intraluminal thrombus and outer wall, layered masks for each slice were carefully reviewed by a physician. Three-dimensional structures were subsequently rendered in Mimics with further iterative smoothing. This process, highlighted in Figure 2, was simple and robust. Masks for the outer wall, intraluminal thrombus, calcifications, lumen, and surrounding bone tissue, when rendered, allowed for the generation of a cohesive three-dimensional image set which portrayed the pathological details of each particular case in proper anatomical context. After observation of the three dimensional isosurfaces, seen in Figure 3, high variability in AAA geometry was apparent from these reconstructed cases, further showing the need for a patient-specific approach. The next section describes results of CFD simulations of blood flow dynamics in ruptured AAAs.

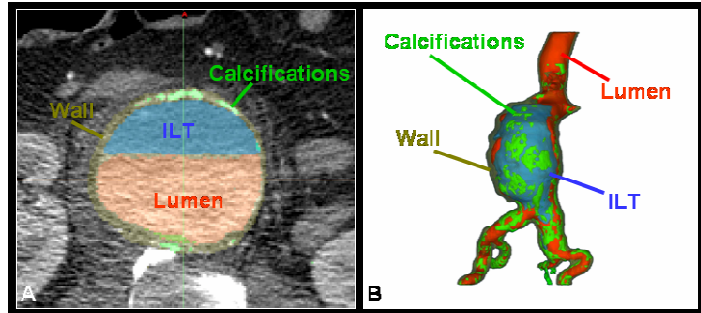


Figure 2. Three dimensional image reconstruction from patient CT data is performed in Mimics using masks for each two-dimensional image slice. (A) Masks are shown in a two dimensional CT image slice. The outer wall is shown in yellow, ILT in blue, calcifications in green, and lumen in red. (B) Three-dimensional rendering of the pathological ruptured structure is performed with further iterative smoothing techniques for each one of the segmented surfaces.

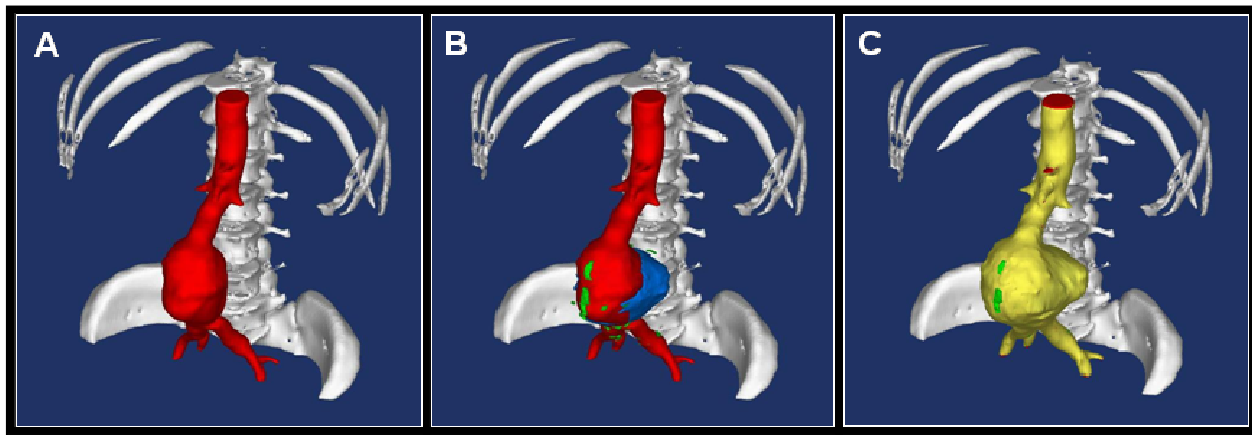


Figure 3. Mimics based rendering of AAA structures depicts the ruptured area below the left vessel at the iliac bifurcation. (A) Lumen of ruptured AAA is shown in red in relation to the skeletal bone structure in white. (B) Calcifications, shown in green, and intraluminal thrombus (ILT), shown in blue, are displayed in relation to the lumen. (C) The outer wall is depicted in yellow surrounding the lumen and ILT.

4. Computational Fluid Dynamics: using an advanced finite volume solver

The reconstructed AAA geometries were imported into an advanced finite volume solver for the analysis of fluid flow dynamics. The fluid material passing through the lumen geometry was modeled as blood with viscosity, $\mu = 0.0035 \text{ kg/m s}$, and density, $\rho = 1050 \text{ kg/m}^3$. The flow was considered laminar. Figure 4 presents the velocity flow field, wall shear stress and the pressure distribution in the blood lumen of the pathological ruptured AAA. The figure shows a distinct pattern of flow recirculation and pressurization of the remodeled vessel. The velocity flow field, in Figure 4A and B, shows recirculation zones around the region of the formed ILT. The wall shear stress distribution of the aneurismal bulge shows a certain circular pattern of increasing shear stress moving towards a central point of high shear stress as seen in Figure 4C. This circular pattern of shear stress undoubtedly is a result of flow recirculation occurring in the region of ILT formation. The magnitude of wall shear stress (WSS) was also observed to be increased around stenotic regions of the vessel above the aneurismal bulge as well as just beyond the iliac bifurcation as shown in reddened regions of the pathological vessel of Figure 4D.

While the study of ruptured AAA geometries, as seen in Figure 4, serves to augment current medical knowledge of the hemodynamic nature of AAAs, more information can be acquired from ruptured AAA geometries through the incorporation of solid features of the vessel. These solid features include the outer wall along with the deposited intraluminal thrombus and calcified plaques. To incorporate both the fluid and solid structures in simulations of AAA geometries serves to improve the quality of information that is provided to the medical professional. Discussion of the incorporation of solid structures in the AAA numerical simulation is provided next.

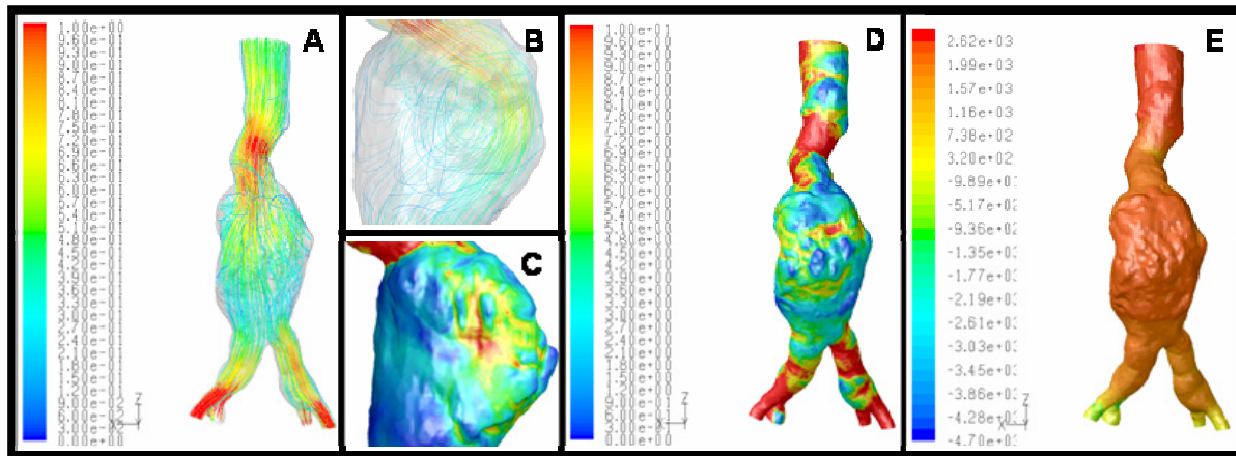


Figure 4. CFD results of a reconstructed AAA lumen geometry. The fluid was considered as blood and the results depict: (A) the pathlines colored by the velocity magnitude, with maximum velocity of $\sim 1\text{m/sec}$. (D) represents the wall shear stress (WSS) acting on the lumen wall. It is observed that the WSS increases drastically at the iliac bifurcation. (E) presents the pressure distribution throughout the pathological lumen geometry. It is observed that the pressure is almost constant throughout the aneurysm. Figures (B) and (C) provide a zoomed view of the aneurismal area where intense recirculation areas are observed along with a location of high WSS.

5. Fluid Structure Interaction approach: calculating stress distribution on the wall

To fundamentally understand the abdominal aortic aneurysm diseases it is important to be able to study the interaction of forces acting between the blood flowing in the lumen and the thin wall surrounding the pathological blood lumen. It is hard for imaging tools to foresee the real hydrodynamics and the conditions of the solid structure under severe disorders like the abdominal aortic aneurysms. The methodology presented in this section will help understanding the

fundamental principles that cause the pathological remodeling of the abdominal aorta. We expect that our FSI models will provide a significant improvement in the understanding of AAA disease.

Fluid flow and blood material properties. The flow is modeled as laminar and transient and blood is considered Newtonian. The equations describing the fluid motion are the Navier-Stokes equations in the arbitrary lagrangian eulerian (ALE) form. This formulation allows the arbitrary grid motion of the fluid domain due to continuous coupling with the thin fibrous wall. The recirculation zones inside the lumen play an important role in the dynamics of the aneurysm and influence the remodeling of the whole structure. It is important to be able to calculate the dynamic interaction of blood inside the lumen with the surrounding solid structures, like the fibrous wall, ILT and calcified spots. Figure 5 shows the computational meshes from the three-dimensional surface structures that originally exported from imaging software and passed through grid generators, to obtain a file format readable for Adina^{11, 13}. The three different computational grids shown from left to right are the blood lumen composed of 32,490 elements, the ILT, 41,895 elements, and the vessel wall, 55,264 elements.

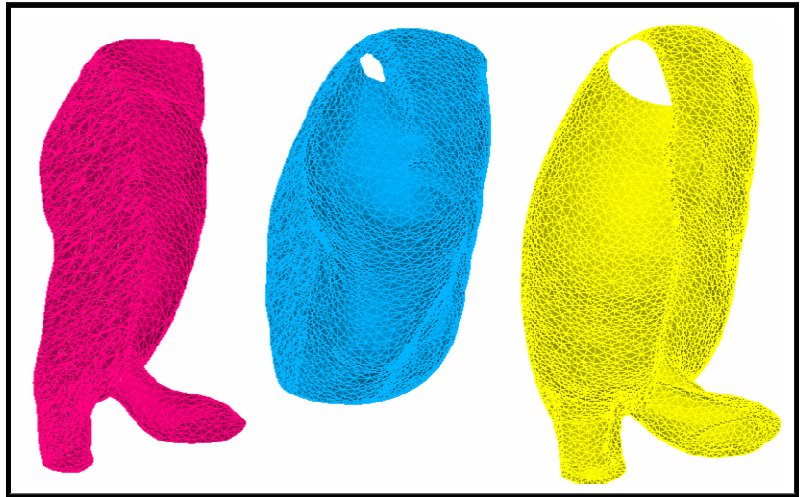


Figure 5. Computational grids generated in Adina, a finite element solver. The three-dimensional surface structures were originally exported from imaging software like Mimics and passed through Gambit, a CFD preprocessor, to obtain a file format readable for Adina. Three different structures are shown from left to right, lumen, ILT, and vessel wall. Through the cross sectional cut, performed in Adina, one can observe the highly tortuous and irregular nature of the pathological vessel of the AAA due to the ILT structure that is attached to the remodeled vessel wall.

Figure 5 shows the computational meshes from the three-dimensional surface structures that originally exported from imaging software and passed through grid generators, to obtain a file format readable for Adina^{11, 13}. The three different computational grids shown from left to right are the blood lumen composed of 32,490 elements, the ILT, 41,895 elements, and the vessel wall, 55,264 elements.

Solid structures– orthotropic formulation – experimental basis. Accurate wall stress analysis of AAA requires information regarding the patient based geometry of the pathological aorta, the wall thickness variability, applied forces acting on the wall and appropriate blood flow conditions. The exact flow rate and pressure at each time of the cardiac pulse is required for the detailed prediction of stress on the AAA wall. To appropriately describe the material properties of the AAA wall, uniaxial testing of abdominal aortic tissue specimens performed by Ragahvan et al.¹⁶, modeled the mechanical behavior of the tissue by using non-linear hyperelastic wall mechanical properties given by the isotropic Mooney-Rivlin formulation¹⁷.

To properly model the mechanical response of AAA tissue, Vande Geest et al.¹⁸ have used tension controlled biaxial testing to characterize the three-dimensional response of the tissue. A high degree of anisotropy in mechanical response was observed between the circumferential and longitudinal directions. Our group fitted experimental data of AAA wall specimens to an exponential strain energy orthotropic material model^{14, 19}. In order to adapt this experimentally observed behavior of AAA wall tissue under mechanical stresses, orthotropic material model developed by Holzapfel et al.²⁰ has been used for multi-layer arterial walls. The Holzapfel strain energy function models the tissue as a fiber-reinforced composite material with the fibers corresponding to the collagenous component of the material. This material formulation was used in many different arterial walls, like aortic walls, coronary arteries, carotid arteries etc.²⁰⁻²⁷ and its mathematical form is shown in equation (1).

$$W = \underbrace{C_1(I_1 - 3) + C_2(I_1 - 3)^2 + D_1(\exp\{D_2(I_1 - 3)\} - 1)}_{\text{isotropic part}} + \underbrace{\frac{k_1}{2k_2} \sum_{i=4,6} \left[2 \exp\{k_2(J_i - 1)^2\} \right]}_{\text{anisotropic}} \quad (1)$$

$$J_4 = C_{ij}(n_a)_i(n_b)_j, \quad J_6 = C_{ij}(n_a)_j(n_b)_i$$

The coefficients in equation (1) used for the fibrous wall and the calcifications are depicted in Table 1. The intraluminal thrombus was modeled as a linear elastic material with Young modulus 110 kPa and Poisson ratio 0.45.

Material	C ₁ [Pa]	C ₃ [Pa]	D ₁ [Pa]	D ₂	k ₁ [Pa]	k ₂	a ^o
Wall	8,888	164,900	48.7	53.46	1,886,000	94.75	5 ^o
Ca	92,000	—	36,000	0.2	—	—	—

FSI Simulation results. FSI simulations to model biomechanical behavior of the AAA wall surrounding the lumen have been performed by several authors²⁸⁻³². However, based on the

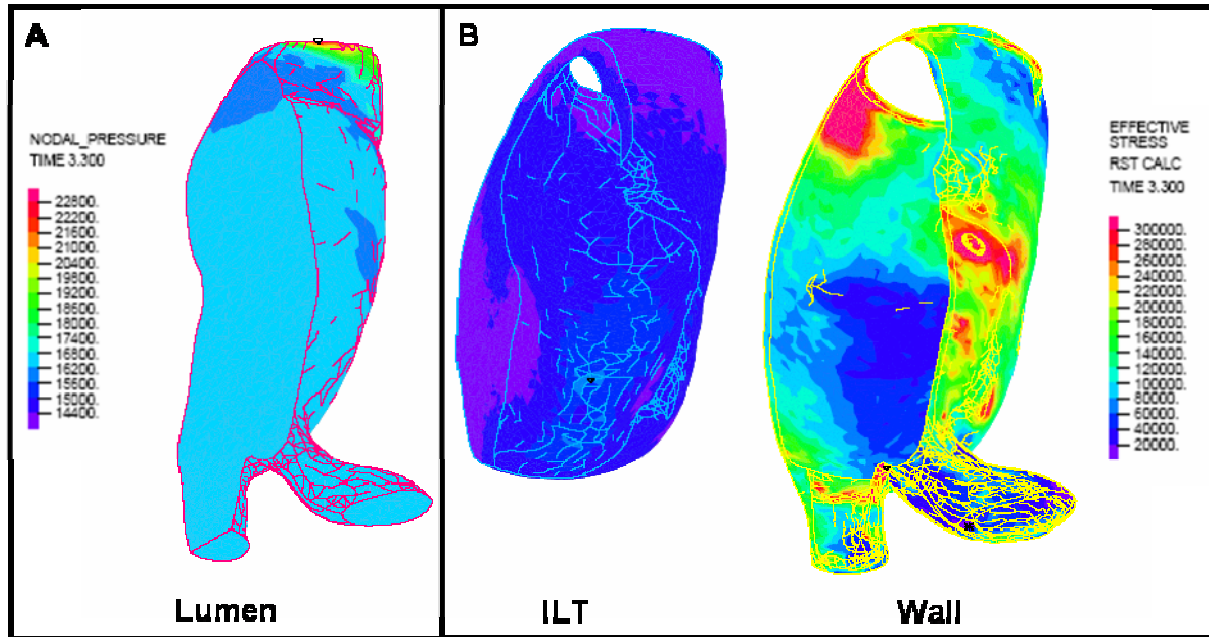


Figure 6. FSI analysis, performed in Adina, allows for the topological determination of stress distribution in the solid structures and pressure field in the fluid domain. (A) The fluid domain pressure distribution depicted in the figure pressurizes the surrounding vessel wall. This effect increases the total stress acting on the AAA structure. (B) The outer wall experiences the highest total stress peaking at ~0.6 MPa at regions where no ILT is present.

isotropic assumption, the directional ambiguities associated with abdominal aortic tissue mechanical response to stresses, which may play a major role in the behavior of the tissue under elevated stresses, cannot be resolved. Our group has used an orthotropic model to determine the wall stress distribution in aneurysms of differing configurations, both with and without thrombus^{14, 15}. The complex flow trajectories within the AAA lumen indicated a possible mechanism for the formation and growth of the intraluminal thrombus (ILT). The resulting magnitude and location of the peak wall stresses was dependent on the shape of the AAA. Our data suggest that while thrombus does not significantly change the location of maximal stress in the aneurysm, the presence of thrombus within the AAA may reduce some of the stress on the wall^{14, 15}. Accordingly, inclusion of calcifications in stress analysis of AAA is important and will increase the accuracy of predicting the risk of AAA rupture³³. As shown in Figure 6 variability of stress is observed based on the structure topology and hemodynamics as described by previous researchers^{34, 35}. The ILT, a much softer

material, accepts lower levels of stress, verifying the notion that it can function as a cushion³⁶. The pressure distribution in the lumen indicated that the blood pressure does not change substantially in the aneurismal area pressurizing the surrounding vessel wall.

Several cases of patients who arrived at the Stony Brook university hospital ER with contained ruptured AAA were studied (where the AAA shape was still contained). In order to test the ability of our models to predict the location of rupture, FSI simulations were performed for one of the above mentioned cases. The results from the FSI simulations indicate highest stresses along the actual rupture line as depicted in Figure 7. In these simulations, the highest stresses occurred on the distal side of the spinal cord and the ILT. For this specific patient AAA configuration, the ILT seemed to offer a significant protective effect by reducing the stresses in the surrounding wall region (purple, figure on the right). Two major locations of stress concentrations were predicted from the FSI simulations, one at the location of the actual rupture and one close to the neck of the aneurysm. The calcifications (green, figure on the left) embedded along the rupture line create regions of high stress concentration (unlike the bigger calcifications that appear deposited, not embedded, on the wall). While indicating that the neck area could have been a potential location for a secondary rupture, the peak stress values (~ 0.5 MPa, occurring at peak systole at $300\mu\text{s}$ from the start of the cardiac cycle) were prominent in the rupture area. The combination of calcifications and a thinner wall observed and extracted from the CT scans in the rupture area above the iliac bifurcation was the most probable contributor to the weakening wall strength where the rupture actually occurred. The FSI simulation clearly captured this, indicating that it would offer a strong predictive value as to the rupture potential for the specific patient.

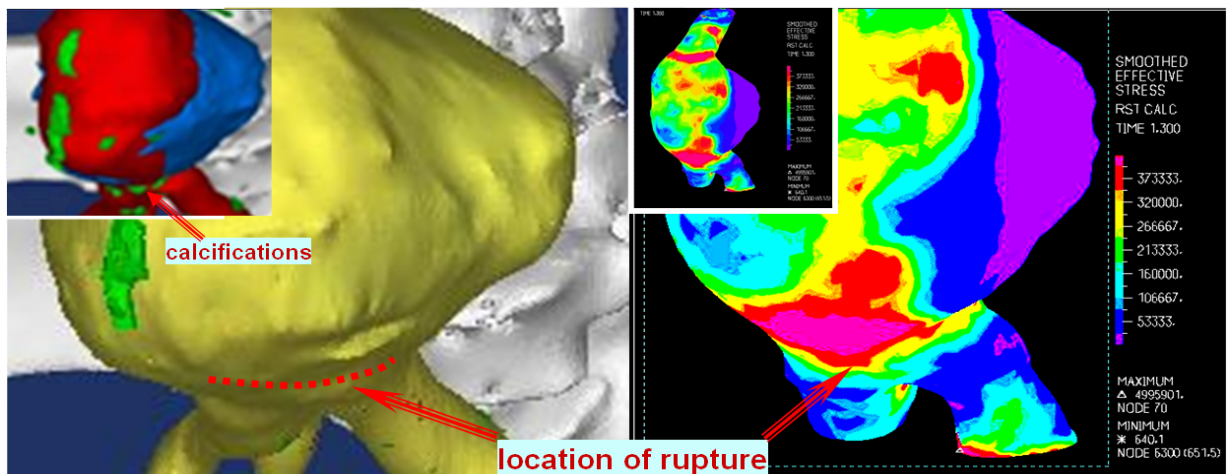


Figure 7. FSI simulation of a ruptured AAA: the location of the maximal wall stresses overlaps the actual rupture region. The inner top panel (left) shows the lumen with calcifications above the bifurcation and the iliac branch. The actual rupture is depicted on the wall surrounding it (yellow). The right panel shows the wall stress contours, with stress concentration along the rupture line.

6. Mimics: a bridge to CFD-FSI

Current imaging modalities can provide qualitative but not quantitative information about blood flow dynamics and wall stresses and strains. The goal of this study is to develop a novel methodology to provide a means of quantifying the risk of rupture of AAAs, through a combination of medical imaging modalities, image reconstruction tools followed by fluid structure interaction (FSI) approaches. The developed FSI approach incorporates advanced constitutive material models of the various components of AAA, including effects of anisotropy due to collagen fiber orientation within the arterial wall, AAA intraluminal thrombus (ILT), and embedded calcifications. With the use of Mimics, the methodology established could ultimately serve as a gateway tool for physicians

and scientists to obtain quantitative information from patient-specific AAA geometries in a non-invasive manner as an extension of current clinical practice. In the future, this methodology will be applicable for analyzing and diagnosing other cardiovascular pathologies, such as vulnerable plaques in carotid and coronary arteries.

References

1. Virmani R, Kolodgie FD, Burke AP, Farb A, Schwartz SM. Lessons from sudden coronary death: a comprehensive morphological classification scheme for atherosclerotic lesions. *Arterioscler Thromb Vasc Biol.* 2000;20(5):1262-1275.
2. Falk E. Why do plaques rupture? *Circulation.* 1992;86(6 Suppl):III30-42.
3. Smith SC, Jr. Risk-reduction therapy: the challenge to change. Presented at the 68th scientific sessions of the American Heart Association November 13, 1995 Anaheim, California. *Circulation.* 1996;93(12):2205-2211.
4. Davies MJ, Thomas AC. Plaque fissuring--the cause of acute myocardial infarction, sudden ischaemic death, and crescendo angina. *Br Heart J.* 1985;53(4):363-373.
5. Powell J, Brady A, Brown L, Forbes J, Fowkes F, Greenhalgh R, Ruckley C. Mortality results for randomised controlled trial of early elective surgery or ultrasonographic surveillance for small abdominal aortic aneurysms. *Thompson SG UK Small Aneurysm Trial Participants, LANCET.* 1998;352:1649-1655.
6. Lederle FA, Wilson SE, Johnson GR, Reinke DB, Littooy FN, Acher CW, Ballard DJ, Messina LM, Gordon IL, Chute EP, Krupski WC, Busuttill SJ, Barone GW, Sparks S, Graham LM, Rapp JH, Makaroun MS, Moneta GL, Cambria RA, Makhoul RG, Eton D, Ansel HJ, Freischlag JA, Bandyk D. Immediate repair compared with surveillance of small abdominal aortic aneurysms. *N Engl J Med.* 2002;346(19):1437-1444.
7. Hua J, Mower WR. Simple geometric characteristics fail to reliably predict abdominal aortic aneurysm wall stresses. *J Vasc Surg.* 2001;34(2):308-315.
8. Fillinger MF, Marra SP, Raghavan ML, Kennedy FE. Prediction of rupture risk in abdominal aortic aneurysm during observation: wall stress versus diameter. *J Vasc Surg.* 2003;37(4):724-732.
9. Wang DH, Makaroun M, Webster MW, Vorp DA. Mechanical properties and microstructure of intraluminal thrombus from abdominal aortic aneurysm. *J Biomech Eng.* 2001;123(6):536-539.
10. *Mimics Medical Imaging Software* [computer program]. Version 12.0. Leuven, Belgium: Materialise, Inc.; 2009.
11. *GAMBIT: Computational Fluid Dynamics Pre-Processor* [computer program]. Version 2.4.6: Ansys Inc.; 2009.
12. *FLUENT: Flow Modeling Software* [computer program]. Version 6.3.26: Ansys Inc.; 2009.
13. *Automatic Dynamic Incremental Nonlinear Analysis* [computer program]. Version 8.5. Watertown, MA: ADINA R&D, Inc.; 2009.
14. Rissland P, Alemu Y, Einav S, Ricotta J, Bluestein D. Abdominal Aortic Aneurysm Risk of Rupture: Patient-Specific FSI Simulations Using Anisotropic Model. *J Biomech Eng.* 2009;131(3):031001-1-10.
15. Bluestein D, Dumont K, De Beule M, Ricotta J, Impellizzeri P, Verheghe B, Verdonck P. Intraluminal thrombus and risk of rupture in patient specific abdominal aortic aneurysm - FSI modelling. *Comput Methods Biomech Biomed Engin.* 2009;12(1):73-81.
16. Raghavan ML, Vorp DA. Toward a biomechanical tool to evaluate rupture potential of abdominal aortic aneurysm: identification of a finite strain constitutive model and evaluation of its applicability. *Journal of Biomechanics.* 2000;33(4):475-482.
17. Mooney M. A theory of large elastic deformation. *Journal of Applied Physics.* 1940;11(9):582-592.
18. Geest JPV, Sacks MS, Vorp DA. The effects of aneurysm on the biaxial mechanical behavior of human abdominal aorta. *Journal of Biomechanics.* 2006;39(7):1324-1334.
19. Vito RP, Hickey J. The Mechanical-Properties of Soft-Tissues .2. The Elastic Response of Arterial Segments. *Journal of Biomechanics.* 1980;13(11):951-957.
20. Holzapfel GA, Gasser TC, Ogden RW. A new constitutive framework for arterial wall mechanics and a comparative study of material models. *Journal of Elasticity.* 2000;61(1-3):1-48.

21. Holzapfel G, Stadler M, Gasser TC. Changes in the mechanical environment of stenotic arteries during interaction with stents: Computational assessment of parametric stent designs. *Journal of Biomechanical Engineering-Transactions of the Asme*. 2005;127(1):166-180.
22. Holzapfel GA, Gasser TC. A viscoelastic model for fiber-reinforced composites at finite strains: Continuum basis, computational aspects and applications. *Computer Methods in Applied Mechanics and Engineering*. 2001;190(34):4379-4403.
23. Holzapfel GA, Gasser TC. Computational stress-deformation analysis of arterial walls including high-pressure response. *International Journal of Cardiology*. 2007;116(1):78-85.
24. Holzapfel GA, Gasser TC, Ogden RW. Comparison of a multi-layer structural model for arterial walls with a fung-type model, and issues of material stability. *Journal of Biomechanical Engineering-Transactions of the Asme*. 2004;126(2):264-275.
25. Holzapfel GA, Gasser TC, Stadler M. A structural model for the viscoelastic behavior of arterial walls: Continuum formulation and finite element analysis. *European Journal of Mechanics a-Solids*. 2002;21(3):441-463.
26. Holzapfel GA, Sommer G, Gasser CT, Regitnig P. Determination of layer-specific mechanical properties of human coronary arteries with nonatherosclerotic intimal thickening and related constitutive modeling. *American Journal of Physiology-Heart and Circulatory Physiology*. 2005;289(5):H2048-H2058.
27. Holzapfel GA, Weizsacker HW. Biomechanical behavior of the arterial wall and its numerical characterization. *Computers in Biology and Medicine*. 1998;28(4):377-392.
28. Di Martino ES GG, Fumero A, Ballerini G, Spirito R, Biglioli P, Redaelli A. Fluid-structure interaction within realistic three-dimensional models of the aneurysmatic aorta as a guidance to assess the risk of rupture of the aneurysm. *Med Eng Phys*. 2001;23:647-655.
29. Fillinger MF, Marra SP, Raghavan ML, Kennedy FE. Prediction of rupture risk in abdominal aortic aneurysm during observation: Wall stress versus diameter. *Journal of Vascular Surgery*. 2003;37(4):724-732.
30. Scotti C, Shkolnik A, Muluk S, Finol E. Fluid-structure interaction in abdominal aortic aneurysms: effects of asymmetry and wall thickness. *BioMedical Engineering OnLine*. 2005;4(1):64.
31. Venkatasubramaniam AK, Fagan MJ, Mehta T, Mylankal KJ, Ray B, Kuhan G, Chetter IC, McCollum PT. A comparative study of aortic wall stress using finite element analysis for ruptured and non-ruptured abdominal aortic aneurysms. *European Journal of Vascular and Endovascular Surgery*. 2004;28(2):168-176.
32. Papaharilaou Y, Ekaterinaris JA, Manousaki E, Katsamouris AN. A decoupled fluid structure approach for estimating wall stress in abdominal aortic aneurysms. *Journal of Biomechanics*. 2007;40(2):367-377.
33. Ricotta JJ, Pagan J, Xenos M, Alemu Y, Einav S, Bluestein D. Cardiovascular disease management: the need for better diagnostics. *Med Biol Eng Comput*. 2008;46(11):1059-1068.
34. Thubrikar MJ, al-Soudi J, Robicsek F. Wall stress studies of abdominal aortic aneurysm in a clinical model. *Ann Vasc Surg*. 2001;15(3):355-366.
35. Thubrikar MJ, Robicsek F, Labrosse M, Chervenkov V, Fowler BL. Effect of thrombus on abdominal aortic aneurysm wall dilation and stress. *J Cardiovasc Surg (Torino)*. 2003;44(1):67-77.
36. Vorp DA. Biomechanics of abdominal aortic aneurysm. *J Biomech*. 2007;40(9):1887-1902.